Dalton Transactions

Accepted Manuscript

ROYAL SOCIETY OF CHEMISTRY

www.rsc.org/dalton

Chemical Science

RSCPublishing

ARTICLE

Binding of pyrazine-functionalized calix[4]arene ligands with lanthanides in an ionic liquid: Thermodynamics and coordination modes†

Cite this: DOI: 10.1039/xoxxoooooox

Received ooth January XXXX,
Accepted ooth January XXXX

DOI: 10.1039/xoxxoooooox

www.rsc.org/

Seraj A. Ansari[a,b], Prasanta K. Mohapatra[b], Willem Verboom[c], Zhicheng Zhang[a] Phuong D. Dau[a], John K. Gibson[a] and Linfeng Rao[a*]

The complexation of representative lanthanides with three calix[4]arenes functionalized with four pyrazine pendent arms containing different substituents such as carbamoyl dioctyl ($\mathbf{L_I}$), diisopropyl phosphonate ($\mathbf{L_{II}}$), and diphenyl phosphoryl ($\mathbf{L_{III}}$) was investigated in water-saturated 1-butyl-3-methylimidazolium bis(trifluoromethanesulfonyl)imide (BumimTf_2N) by absorption spectroscopy, luminescence spectroscopy, and microcalorimetry. All three ligands form 1:1 ML complexes (M = Eu^{3+}, and L = ligand), and the stability constants (log β) follow the order: $\mathbf{L_I}$ (-1.38 ± 0.66) << $\mathbf{L_{II}}$ (3.71 ± 0.02) < $\mathbf{L_{III}}$ (7.47 ± 0.03), similar to the trend in the metal distribution coefficients in the solvent extraction using these ligands as extractants. The enthalpy of complexation, determined by microcalorimetry, show that the complexation of lanthanides with these bulky ligands is exothermic, and proceeds via replacement of water molecules from the primary coordination spheres. The 1:1 stoichiometry of the ML complexes was confirmed by electrospray ionization mass spectrometry. Results from optical absorption, luminescence and ^{31}P-NMR spectroscopy suggest that, out of four pendent arms on the rigid calixarene platform, only two arms coordinate with the lanthanide ion and each arm is tridentate. The influence of structural features of the ligand on the complexation of lanthanides is explained with the help of thermodynamic parameters.

Introduction

Calix[4]arenes have been widely employed as a rigid platform for the synthesis of pre-organized molecules to enhance their molecular and ionic recognition, and in many other domains of supramolecular chemistry.[1] In fact, the high level of pre-organization, and the now well understood conformational behavior of calix[4]arenes, have boosted the development of calixarene-based extractants with high efficiency and selectivity.[2] The attachment of single monodentate ligand units to a rigid scaffold like calix[4]arene results in multi-dentate ligands with a certain degree of pre-organization and a high degree of complexation compared to the bare single ligand. Attachment of multidentate ligands, including the bidentate CMPO (carbamoyl methylene phosphine oxide) and malonamide-based ligands, and tridentate diglycolamide ligands that have recently been applied to the extraction of trivalent lanthanides (Ln) and actinides (An) which are non-extractable with the conventional monodentate tri-*n*-butyl phosphate (TBP),[3,4] could further enhance the binding strength and selectivity. As a result, attempts have been made to functionalize these ligands on a rigid platform such as calix[4]arenes or on a tripodal platform.[5-11] In all cases, significant enhancements in the extraction ability of the ligands have been observed.

The Ln/An group separation is still one of the most challenging chemical processes due to the similar chemical properties of the two group elements. Because the 5*f*-orbitals are more extended and have a higher tendency to participate in chemical bonding than the 4*f*-orbitals, the extractants containing softer donor atoms (*N* or *S*) have shown higher affinity for the actinides.[12] This has been the basis for a number of recent developments of extractants for Ln/An separation, including heterocyclic multiple nitrogen donor ligands that have been successfully tested for Ln/An separation from 2 M nitric acid solutions,[13] and a series of pre-organized picolinamide functionalized calix[6]arene ligands.[14] Though the separation factor for An and Ln metal ions by the picolinamide-functionalized calix[6]arene ligands was not high, the studies have indicated that decreasing the basicity of the pyridine unit could help to improve the selectivity. For example, it is known that the basicity of the nitrogen atoms in pyrazine are lower than that of the nitrogen in pyridine, and it has been shown that appropriately functionalized water-soluble pyrazine-based ligands exhibit good selectivity and affinity towards americium over europium in nitric acid solution.[15] Taking advantages of the calixarene platform that facilitates the pre-organization of functional ligands, a series of pyrazine-functionalized calix[4]arene ligands have been prepared and tested for the separation of Ln and An.[16] However, lack of fundamental understanding of the metal-ligand complexation often causes difficulties to understand the separation processes in solvent extraction, where the complexation process is the first step before the transfer of the metal-ligand complex into the water immiscible organic phase.

To help the development of more effective separation processes, in the present study, we investigated the thermodynamics

and coordination modes in the complexes of Eu^{3+} with three calix[4]arenes appended with four pyrazine pendent arms containing substituents including carbamoyl dioctyl (**L_I**), diisopropyl phosphonate (**L_{II}**), and diphenyl phosphoryl (**L_{III}**) (Fig. 1) in an ionic liquid (IL) medium. The ionic liquid, 1-butyl-3-methylimidazolium bis(trifluoromethane-sulfonyl)imide ($BumimTf_2N$), was used as an alternate solvent to hazardous solvents such as nitrobenzene that was used in previous solvent extraction experiments.[16] Ionic liquids have been widely explored as an alternate "green" solvent for the separation of metal ions containing various extractants, and offer several advantages as alternative diluents such as low volatility, amazing ability to dissolve organic and inorganic compounds and their tunability.[17,18] Eu^{3+} was chosen as a representative lanthanides due to its luminescence properties. The results of this study will help to gain fundamental knowledge on metal-ligand interactions in the separation processes using these ligands as extractants in the ionic liquid medium.

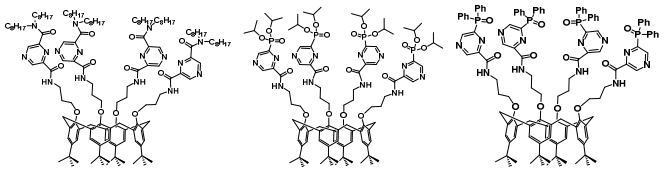

L_I **L_{II}** **L_{III}**

Fig. 1. Structural formulae of pyrazine-functionalized calix[4]arene ligands containing different substituents: carbamoyl dioctyl (**L_I**), diisopropyl phosphonate (**L_{II}**), and diphenyl phosphoryl (**L_{III}**). The bond angles around the pyrazines do not represent the actual angles for clarity of the figures.

Results

Stability constants of Eu^{3+}/ligand complexes: spectrophotometry

Prior to the spectrophotometric titrations to study the complexation of Eu^{3+} with the ligands, the absorption spectra of **L_I**, **L_{II}**, and **L_{III}** were recorded in the wavelength region of 200 – 800 nm to identify appropriate absorption bands to be used in spectrophotometric titrations. As shown in Fig. 2, all three ligands show strong absorption bands at 256 and 301 nm. An additional absorption band at 333 nm for **L_{II}** and at 338 nm for **L_{III}** was also observed, while the absorption band of **L_I** between 333 – 338 nm was very weak. Further analysis using ligand solutions of different concentrations indicated that, for all three ligands, the absorption bands in the wavelength region of 285 nm - 400 nm followed Beer's Law and are suitable for spectrophotometry, while the intensities of the absorption band at 256 nm were not dependent on the ligand concentration (0.05 - 0.50 mmol/L) (Fig. S1 in SI). Based on these results, only the absorption spectra in the wavelength region of 285 – 400 nm were used to determine the stability constants of Eu^{3+}/ligand complexes.

Fig. 3 (left figure) shows representative spectrophotometric titrations of **L_{II}** and **L_{III}** with Eu^{3+} in $BumimTf_2N$. As Eu^{3+} was added into the ligand solution, the intensity of the absorption band at 300 nm increased with simultaneous decrease in the intensity of the absorption band at 340 nm. Little change in the absorption bands was observed when the metal to ligand ratio (C_{Eu}/C_L) was beyond 1.4, implying a limiting complex had been achieved. Factor analysis of the spectra by the Hypspec program[19] suggested that there were two absorbing species, the free ligand and the ML complex, and the best fit was achieved by using the model of the formation of 1:1 complex, $Eu(L)^{3+}$. The calculated molar absorptivities of the free ligands and the Eu^{3+}/ligand complexes are shown in Fig. 3 (right Figure).

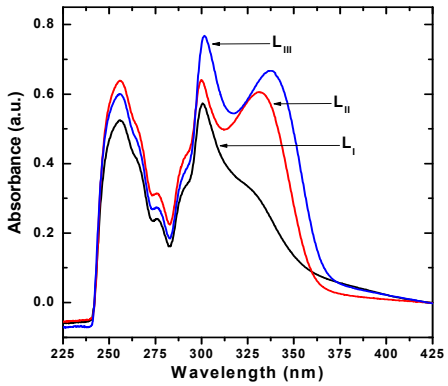

Fig. 2. Absorption spectra of pyrazine-functionalized calix[4]arene ligands, **L_I**, **L_{II}**, and **L_{III}**, in $BumimTf_2N$; Ligand concentration: 0.25 mmol/L; Temperature: 25 °C.

The stability constants of the $Eu(L)^{3+}$ complexes are shown in Table 1. Similar titrations were also conducted with **L_I**, but the changes in the absorption spectra were quite small as Eu^{3+} was added into the ligand solution (Fig. S2 in SI). This indicates that the complexation of Eu^{3+} with **L_I** is much weaker than that with **L_{II}** and **L_{III}**. Nevertheless, the spectra could be fitted by the HypSpec program to obtain the stability constant of $Eu(L_I)^{3+}$ complex. The value, with a larger uncertainty, is also listed in Table 1 for comparison. The stability constants of the Eu^{3+} complexes with **L_{II}** and **L_{III}** were also determined at different temperatures (25 - 60 °C) to evaluate the effect of temperature on the complexation. The spectra at different temperatures were similar to those at 25 °C shown in Fig. 3. The stability constants, calculated with HypSpec and summarized in Table 1, indicate that the complexation becomes weaker at higher temperatures for both ligands.

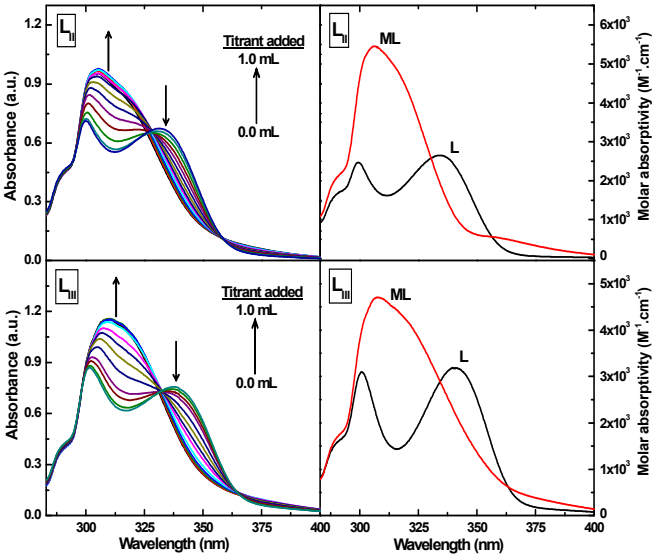

Fig. 3. Spectrophotometric titration of **L_{II}** and **L_{III}** with $Eu(Tf_2N)_3$ (Left), and deconvoluted spectra of ligands (L) and metal/ligand complexes (ML) (right). Cuvette solution: 0.25 mmol/L ligands (0.8 mL); Titrant: 3.8 mmol/L $Eu(Tf_2N)_3$ added in the range of 0.01 – 1.0 mL; Temperature: 25 °C.

Table 1. Thermodynamic data for the complexation of Eu^{3+} with pyrazine-functionalized calix[4]arene ligands in $BumimTf_2N$

Equilibrium	T (°C)	K_d [a]	Log β	ΔH (kJ/mol)	ΔS (J/mol/K)
$Eu^{3+} + \mathbf{L_I} = Eu(\mathbf{L_I})^{3+}$	25	0.01	−1.38 ± 0.66		
$Eu^{3+} + \mathbf{L_{II}} = Eu(\mathbf{L_{II}})^{3+}$	25	5.5 ± 0.3	3.71 ± 0.02	−10.9 ± 1.1 [b]	35 ± 3
				−12.7 ± 1.8 [c]	28 ± 3
	40		3.60 ± 0.02		
	50		3.53 ± 0.01		
	60		3.48 ± 0.02		
$Eu^{3+} + \mathbf{L_{III}} = Eu(\mathbf{L_{III}})^{3+}$	25	135 ± 8.5	7.47 ± 0.02	−12.1 ± 2.1 [b]	102 ± 15
				−14.8 ± 1.9 [c]	93 ± 11
	40		7.33 ± 0.04		
	50		7.27 ± 0.02		
	60		7.19 ± 0.02		

[a] K_d for the two-phase equilibrium in extraction: $Eu_{aq}^{3+} + L_{IL} = EuL_{IL}^{3+}$, aqueous phase: 1 mol/L HNO_3, IL phase contained 0.1 mmol/L ligand; [b] by calorimetry; [c] by spectrophotometry

Distribution coefficients in solvent extraction

The K_d values of the distribution of Eu^{3+} between the IL phase (0.1 mmol/L ligand) and the aqueous phase (1 mol/L HNO_3) are shown in Table 1. The data show that the extractability of Eu^{3+} follows the order: $\mathbf{L_I} << \mathbf{L_{II}} < \mathbf{L_{III}}$. To identify the stoichiometry of the extracted species, the K_d was measured at varying ligand concentrations (0.01 – 0.1 mmol/L) and fixed nitrate concentration (1 mol/L HNO_3). The slope analysis of the extraction data, log K_d vs. log [L] (Fig. S3 in SI), indicates that the extracted species has a stoichiometry of 1:1 ratio for Eu^{3+}/L, suggesting the formation and extraction of $Eu(L)^{3+}$ complex into the $BumimTf_2N$ phase as described by equilibrium reaction (1), where the subscripts "aq" and "IL" denote the aqueous or $BumimTf_2N$ phases, respectively.

$$Eu_{aq}^{3+} + L_{IL} = EuL_{IL}^{3+} \qquad (1)$$

Enthalpy of complexation: microcalorimetry

Fig. 4 shows representative calorimetric titrations of Eu^{3+} with $\mathbf{L_{II}}$ and $\mathbf{L_{III}}$. The enthalpies of complexation were calculated from the reaction heat by the Hyperquad program,[20] and listed in Table 1. The complexation of Eu^{3+} with both $\mathbf{L_{II}}$ and $\mathbf{L_{III}}$ is exothermic. It was not possible to determine the enthalpy of complexation with $\mathbf{L_I}$ by calorimetry because the complexation is too weak as shown by spectrophotometry.

Luminescence spectra and lifetime of Eu^{3+} complexes

Fig. 5(a) shows representative luminescence spectra of Eu^{3+} in the presence of $\mathbf{L_{II}}$ in $BumimTf_2N$. The spectra contain features originating from electronic transitions from the lowest excited state of Eu^{3+}, $^5D_0$, to the ground state manifold, $^7F_1$ (592 nm), $^7F_2$ (613 nm) and $^7F_4$ (692 nm). As the ligand concentration was increased from 0 to 10 mmol/L, changes occurred in the transitions of $^5D_0 \rightarrow {}^7F_1$, $^5D_0 \rightarrow {}^7F_2$, and $^5D_0 \rightarrow {}^7F_4$, indicating the perturbation of the primary coordination sphere of Eu^{3+} by the ligand. In particular, the intensity of the hypersensitive $^5D_0 \rightarrow {}^7F_2$ transition (around 610-620 nm) increased significantly with increased ligand concentration, indicating changes in the coordination environment around the central Eu^{3+} ion. A plot of the peak intensity at 613 nm as a function of C_L/C_{Eu} (Fig. 5b) shows that the intensity increased gradually up to the C_L/C_{Eu} ratio of 1.4, and remained nearly constant thereafter, indicating the completion of the complexation reaction. This behavior is in line with the formation of $Eu(L)^{3+}$ species that was 90% complete at this ratio of C_L/C_{Eu}, as shown by the speciation diagram in Fig. 5b.

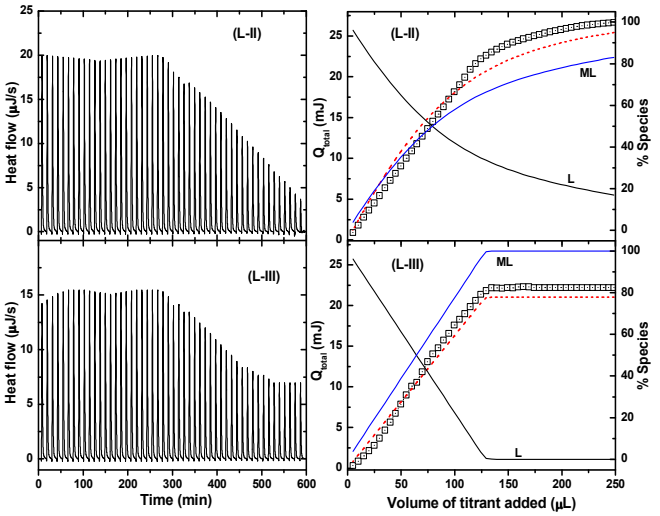

Fig. 4. Representative calorimetric titration of $Eu(Tf_2N)_3$ with $\mathbf{L_{II}}$ and $\mathbf{L_{III}}$. Left: thermograms (uncorrected for dilution heat). Right: cumulative heat and speciation of Eu^{3+} as a function of the titrant volume. (□) experimental heat, ---- fitted heat, — percentages of Eu^{3+} species. C_L (titrant) = 5.3 mmol/L for $\mathbf{L_{II}}$ or 4.8 mmol/L for $\mathbf{L_{III}}$; Initial cup solution: 0.50 μmol $Eu(Tf_2N)_3$ (for $\mathbf{L_{II}}$) or 0.64 μmol $Eu(Tf_2N)_3$ for ($\mathbf{L_{III}}$).

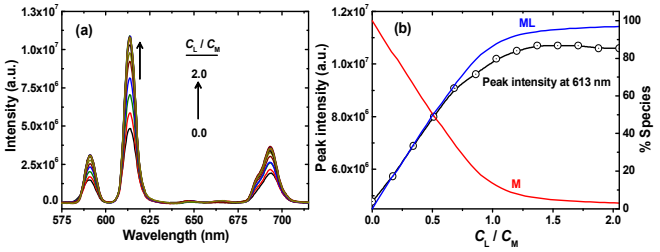

Fig. 5. Luminescence titration of $Eu(Tf_2N)_3$ with $\mathbf{L_{II}}$. (a) Emission spectra; (b) Intensity of the emission band at 613 nm and the speciation of Eu^{3+} as a function of C_L/C_{Eu}. Excitation wavelength: 395 ± 5 nm; Emission wavelength: 612 ± 5 nm. Cuvette solution: 15 mmol/L $Eu(Tf_2N)_3$ (1.5 mL); Titrant: 15.3 mmol/L $\mathbf{L_{II}}$.

Table 2. Luminescence lifetime for the complexation of Eu^{3+} with $\mathbf{L_{II}}$ in $BumimTf_2N$, and the calculated hydration number

C_L/C_{Eu}	τ (μs)	N_{H2O} (± 0.5)
0	106	9.2
0.17	114	8.5
0.34	122	7.9
0.51	134	7.1
0.68	168	5.6
0.86	183	5.0
1.03	188	4.9
1.20	251	3.5
1.37	311	2.7
1.54	298	2.8
1.71	309	2.7
1.88	329	2.5
2.05	296	2.8

The luminescence decay of Eu^{3+} in $BumimTf_2N$ (Fig. S4 in SI) indicated that in the absence of ligands, the lifetime of Eu^{3+} in the water saturated $BumimTf_2N$, 106 μs, was very close to those of Eu^{3+} in water, 113 μs from this work and 108 μs in the literature,[21] implying that the primary coordination sphere of Eu^{3+} in the water saturated $BumimTf_2N$ is identical to that in water, i.e., $N_{H2O} \approx 9$. The luminescence lifetime became longer as the concentration of the ligand was increased, indicating the replacement of water molecules from the primary coordination sphere of Eu^{3+} ion. As the C_L/C_{Eu} ratio achieved 1.4 and beyond, no further change in the luminescence decay rate was observed (Fig. S4 in SI), indicating the completion of the complexation reaction. From the luminescence lifetime, the number of water molecules present in the primary coordination sphere of Eu^{3+} was calculated using the equation: $N_{H2O} = (1.05 \times 10^3)/\tau - 0.7$, where τ is the lifetime (μs),[21] and shown in Table 2.

Discussion

Trends in the binding strength of $\mathbf{L_I}$, $\mathbf{L_{II}}$ and $\mathbf{L_{III}}$ with Eu^{3+}: Correlation with distribution coefficients in solvent extraction

The stability constants of the $Eu(L)^{3+}$ complexes in Table 1 show that the binding strength of the three pyrazine-functionalized calixarene ligands follows the order: $\mathbf{L_I} << \mathbf{L_{II}} < \mathbf{L_{III}}$. This means that, the nature of the substituents on the pyrazine moiety has a significant effect on the binding strength: $\mathbf{L_I}$ with the carbamoyl dioctyl group is the weakest, $\mathbf{L_{II}}$ with the diisopropyl phosphonate group is stronger, and $\mathbf{L_{III}}$ with the diphenyl phsophoryl group is the strongest. This trend could probably be interpreted by the difference in the basicity of the functional groups and the steric effects of the ligands. On one hand, the stronger complexation of $\mathbf{L_{III}}$ with Eu^{3+} than $\mathbf{L_{II}}$ is due to the higher basicity of the diphenyl phosphoryl oxygen than the oxygen of the diisopropyl phosphonate group, since it is known that phosphine oxide is more basic than phosphonate. On the other hand, the planar phenyl group in $\mathbf{L_{III}}$ causes less steric crowding around the ligating phosphoryl group compared to that of the bulky secondary isopropyl groups attached to the P=O moieties in $\mathbf{L_{II}}$. As a result, ligand $\mathbf{L_{III}}$ could approach the Eu^{3+} ion more closely to form a stronger complex. In addition, the presence of the large octyl groups in $\mathbf{L_I}$ results in the distortion in the pre-organized structure of the ligands on the calixarene platform, twisting the coordination sites away from one another, resulting in the weakest complexation between $\mathbf{L_I}$ and Eu^{3+}. The trend in the stability constants of the $Eu(L)^{3+}$ complexes is, in fact, in good agreement with the order of the distribution coefficients in solvent extraction. As shown in Table 1, the K_d values follows the order: 0.01 ($\mathbf{L_I}$) < 5.5 ($\mathbf{L_{II}}$) < 135 ($\mathbf{L_{III}}$). The agreement suggests that, among a number of steps in the solvent extraction process, the formation of the $Eu(L)^{3+}$ complex is probably the most important step in determining the overall energetics of extraction.

Effect of temperature: Energetics of the complexation in IL

Fig. 6 shows the van't Hoff plot for the stability constants of the $Eu(L)^{3+}$ complexes (L = $\mathbf{L_{II}}$ and $\mathbf{L_{III}}$) at different temperatures. The data could be well represented by linear correlations between $\ln\beta$ and 1/T, suggesting that the enthalpy of complexation could be considered constant in the temperature range of 25 °C to 60 °C, and the enthalpy of complexation can be calculated from the slopes of the linear fits. The enthalpies of complexation calculated from the van't Hoff plot, –(12.7 ± 1.8) kJ/mol for EuL_{II}^{3+} and –(14.8 ± 1.9) kJ/mol for EuL_{III}^{3+}, overlap with the enthalpies of complexation directly determined at 25°C by microcalorimetry, –(10.9 ± 1.1) kJ/mol for EuL_{II}^{3+} and –(12.1 ± 2.1) kJ/mol for EuL_{III}^{3+}, within the 95% confidence levels. The entropies of complexation were accordingly calculated from the Gibbs free energy and enthalpy ($\Delta G = \Delta H - T\Delta S$) and listed in Table 1. Evidently, the complexation of Eu^{3+} with $\mathbf{L_{II}}$ and $\mathbf{L_{III}}$ is both enthalpy and entropy driven. The positive entropy of complexation probably reflects the increase in the degree of disorder due to the release of water molecules from the primary coordination spheres of Eu^{3+} and the ligand. This will be further discussed in conjunction with the luminescence data in the later section.

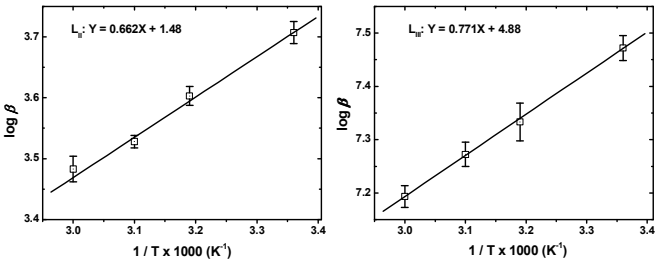

Fig. 6. van't Hoff plots for the complexation of Eu^{3+} with $\mathbf{L_{II}}$ and $\mathbf{L_{III}}$.

Characterization of Eu^{3+}/ligand complexes

Results from multiple techniques, including ESI-MS, luminescence, and ^{31}P-NMR spectroscopy, helped to confirm the stoichiometry of the complex, and reveal the coordination mode of the ligand in the Eu^{3+} complex in $BumimTf_2N$. In these experiments, the complex of Eu^{3+} with $\mathbf{L_{II}}$ was studied and the results are discussed as follows.

Stoichiometry. Fig. 7 shows the results of ESI-MS experiments. The $Eu(L_{II})^{3+}$ species, besides the cation and anion of the ionic liquid medium ($Bumim^+ \cdot Tf_2N^-$), was clearly identified in ESI-MS spectra. This corroborates very well with the results of spectrophotometry and solvent extraction.

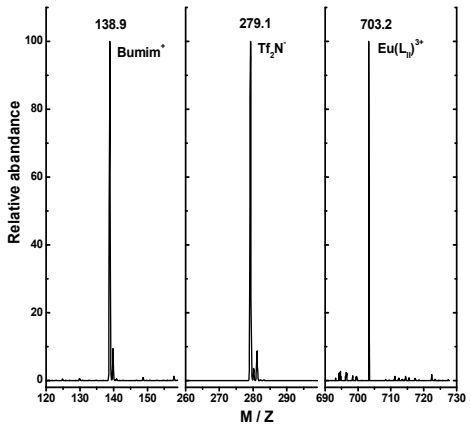

Fig. 7. ESI-MS spectrum of the species in BumimTf$_2$N

Coordination number and mode. Fig. 8 shows the hydration number, calculated from the luminescence lifetime in Table 2, as a function of the C_L/C_{Eu} ratio. As shown by the speciation diagram of Eu^{3+} in Fig. 8, at $C_L/C_{Eu} \approx 1.2$, the formation of the $Eu(L)^{3+}$ complex was nearly completed, and the hydration number of Eu^{3+} remained constant at $N_{H2O} \approx 3$. This implies that the remaining 6 out of 9 coordination sites of Eu^{3+} are occupied by the donor atoms of the ligand. Since each of the four pendent pyrazine arm in $\mathbf{L_{II}}$ contains three potential donor atoms: *O* (from carbonyl), *N* (from pyrazine), and *O* (from phosphoryl), the possibility of all of them participating in the binding with Eu^{3+} ion is excluded by the luminescence data. A reasonable hypothesis is that, out of the four pendent arms, only two arms are positioned in such a manner that allows its three donor atoms to coordinate with Eu^{3+} that is in the center of the cavity (each of the two coordinating arms is tridentate). In contrast, the other two pendent arms probably bend away from the center of the cavity, not participating (or only weakly participating) in the binding. The results from ^{31}P-NMR (using lanthanum instead of europium) validated this hypothesis.

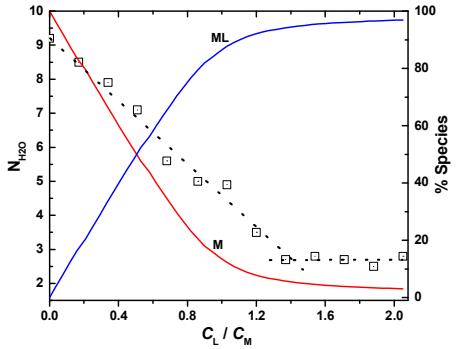

Fig. 8. Variation of N_{H2O} (□, left y-axis) and ML speciation (solid lines, right y-axis) as functions of C_L/C_M ratio. L refers to $\mathbf{L_{II}}$ and M refers to Eu^{3+}.

Fig. 9 shows the ^{31}P-NMR spectra of free $\mathbf{L_{II}}$ (in the absence of La(III)) and the La(III)/$\mathbf{L_{II}}$ complex. The ^{31}P-NMR spectra of the pure ligand showed only a single peak, as all the P atoms are equivalent in the ligand. However, the peak split into two and the chemical shift was moved down-field due to the de-shielding caused by the sharing of its electron density with the metal ion. The presence of two types of P atoms with almost identical intensity is an indication that the four pendent arms in the $La(L_{II})^{3+}$ complex are not identical. It is very likely that the phosphoryl groups on two arms are strongly bonded with La^{3+}, and the phosphoryl groups on the other two arms are either not bonded or very weakly bonded (outer sphere) with the metal ion.

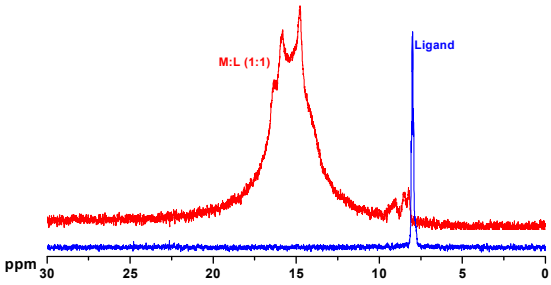

Figure 9. ^{31}P-NMR spectrum of the $\mathbf{L_{II}}$ ligand and the $La(L_{II})^{3+}$ complex.

Based on the ESI-MS, luminescence and NMR data, the structure of the Eu^{3+} complexes with the pyrazine-functionalized ligands, $\mathbf{L_{II}}$ and $\mathbf{L_{III}}$ for example, could be best represented by Fig. 10.

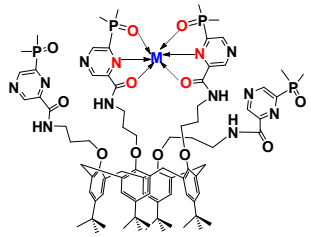

Fig. 10. Probable structure of an M/L complex in BumimTf$_2$N. Coordinating water molecules ($N_{H2O} \approx 3$) are omitted for clarity.

Conclusions

The thermodynamic parameters and coordination modes of the Eu^{3+} complexes with three calix[4]arene ligands appended with four pyrazine pendent arms containing substituents such as carbamoyl dioctyl ($\mathbf{L_I}$), diisopropyl phosphonate ($\mathbf{L_{II}}$), and diphenyl phosphoryl ($\mathbf{L_{III}}$) in water-saturated BumimTf$_2$N was investigated. All three ligands formed 1:1 ML complex and the stability constants (log β) followed the order: $\mathbf{L_I}$ (−1.38 ± 0.66) < $\mathbf{L_{II}}$ (3.71 ± 0.02) < $\mathbf{L_{III}}$ (7.47 ± 0.03), implying that the nature of the substituents on the pyrazine moiety has a significant effect on the binding strength. The complexation of lanthanides with these bulky ligands is exothermic, and proceeds via the replacement of water molecules from the primary coordination sphere of the metal ion. Based on the data from optical absorption, luminescence, electrospray ionization mass spectrometry and ^{31}P-NMR spectroscopy, it was concluded that in 1:1 metal-ligand complex, two pendent arms of the ligand coordinate to Eu^{3+} in a tridentate mode, and the other two arms are either non-bonded or very weakly bonded (outer sphere) with the metal ion.

Experimental

Pyrazine-functionalized calix[4]arene ligands ($\mathbf{L_I}$, $\mathbf{L_{II}}$ and $\mathbf{L_{III}}$, Fig. 1) were synthesized by coupling appropriately substituted pyrazines on a calixarene platform via a palladium-catalyzed cross-coupling reaction described previously.[16] The ionic liquid, $BumimTf_2N$, was procured from Sigma Aldrich (CAS 174899-83-3), and equilibrated with an equal volume of Milli-Q water before use. The water content of the $BumimTf_2N$ was calculated to be about 1 mol/L.[22] The $Eu(Tf_2N)_3$ salt was prepared by the reaction of its oxide with trifluoromethane sulfonimide (Sigma Aldrich) based on the procedures in the literature.[23] A stock solution of $Eu(Tf_2N)_3$ was prepared by dissolving an appropriate amount of the salt in IL, and standardized by EDTA titration.

Absorption spectra of the ligands were collected in the wavelength region of 225 - 425 nm (0.1 nm interval) on a double beam Varian Cary-5G spectrophotometer using 10 mm path length quartz cells. The temperature of the sample and reference cell holders was controlled by water circulation from a thermostated water bath. In each titration, appropriate aliquots of titrant were added into the cell and mixed thoroughly for about 5 minutes before the spectrum was recorded. The mixing time was found to be sufficient to complete the complexation reaction. Usually 15 - 20 spectra were recorded in each titration. The stability constants of the Eu^{3+}/ligand complexes were calculated by nonlinear least-squares regression analysis using the HypSpec program.[19] The details about the luminescence emission spectra and lifetime of Eu^{3+} in aqueous and in $BumimTf_2N$ have been previously described.[24]

Microcalorimetric titrations were performed on an isothermal titration microcalorimeter (TAM-III) and the detail procedure is described elsewhere.[24] The titrations were performed by adding the ligand solution, in 5 µL additions through a 250 µL Hamilton syringe, into the reaction vessel that initially contained 750 µL solution of $Eu(Tf_2N)_3$ in $BumimTf_2N$. About 50 additions of the titrant were made in each experiment. The reaction heat was then used, in conjunction with the stability constants, to calculate the enthalpy of complexation with the HypDeltaH program.[20]

The Electrospray Ionization Mass Spectrometry (ESI-MS) experiments were performed using an Agilent 6340 quadrupole ion trap mass spectrometer with a micro-ESI source. The metal/ligand complex was prepared by mixing a known amount of $\mathbf{L_{II}}$ and $Eu(Tf_2N)_3$ in $BumimTf_2N$ at C_L/C_M ratio ≈ 4. The complex was then diluted with acetonitrile (HPLC grade) for injecting directly into the ESI capillary at a flow rate of 1 µL/min. Typical concentrations of the analytes in the spray solution were: ~30 µmol/L ligand, ~8 µmol/L Eu^{3+}, ~55 µmol/L Tf_2N^-, and ~30 µmol/L C_4mim^+. Depending on the chosen polarity (positive or negative), all the positive and negative charged species were detected, respectively.

The ^{31}P-NMR spectra of the La^{3+}/ligand ($\mathbf{L_{II}}$) complexes were recorded in deuterated acetonitrile medium at 120 MHz. The La^{3+} ion was chosen as a representative lanthanide because it is not paramagnetic. Deuterated acetonitrile was chosen as the medium due to two reasons: (1) it was very difficult, if not impossible, to obtain the NMR spectra using $BumimTf_2N$ as the medium because its ionic charges caused serious interference with the applied magnetic field; and (2) acetonitrile is known to be a very weakly solvating agent, similar to the ionic liquid. The sample was prepared by dissolving a known amount of ligand and $La(ClO_4)_3$ in deuterated acetonitrile (1:1 mole ratio). The ^{31}P-NMR spectra of both the free ligand sample (without La^{3+}) and the La(III)/Ligand complex were recorded.

Acknowledgements

This work was supported by the Director, Office of Science, Office of Basic Energy Science of the U.S. Department of Energy (DOE), under Contract No. DE-AC02-05CH11231 at LBNL. SAA acknowledges the Indo-US Science & Technology Forum (IUSSTF) for awarding a fellowship.

Notes and references

[a] Chemical Sciences Division, Lawrence Berkeley National Laboratory, Berkeley, California 94720, USA. E-mail: LRao@lbl.gov.
[b] Radiochemistry Division, Bhabha Atomic Research Centre, Mumbai 400085, India.
[c] *Laboratory of Molecular Nanofabrication, Institute for Nanotechnology, University of Twente, P.O. Box 217, 7500 AE Enschede, The Netherlands*
†Electronic Supplementary Information (ESI) available: [Figures S1-S4]. See DOI: 10.1039/b000000x/

1 A. Ikeda and S. Shinkai, *Chem. Rev.*, 1997, **97**, 1713.
2 B. S. Creaven, D. F. Donlon and J. McGinley, *Coord. Chem. Rev.*, 2009, **253**, 893.
3 S.A. Ansari, P.N. Pathak, P.K. Mohapatra and V.K. Manchanda, *Chem. Rev.*, 2012, **112**, 1751.
4 S.A. Ansari, P.N. Pathak, P.K. Mohapatra and V.K. Manchanda, *Sep. Purif. Rev.*, 2011, **40**, 43.
5 V.A. Babain, M.Y. Alyapyshev, M.D. Karavan, V. Bohmer, L. Wang, E.A. Shokova, A.E. Motornaya, I.M. Vatsouro and V.V. Kovalev, *Radiochim. Acta*, 2005, **93**, 749.
6 P.K. Mohapatra, A. Sengupta, M. Iqbal, J. Huskens and W. Verboom, Inorg. Chem., 2013, 52, 2533−2541.
7 M. Iqbal, P.K. Mohapatra, S.A. Ansari, J. Huskens and W. Verboom, *Tetrahedron*, 2012, **68**, 7840.
8 M. Karavan, F. Arnaud-Neu, V. Hubscher-Bruder, I. Smirnov and V. Kalchenko, *J. Inclusion Phenom. Macrocyclic Chem.*, 2010, **66**, 113.
9 O. Klimchuk, L. Atamas, S. Miroshnichenko, V. Kalchenko, Smirnov, V. Babain, A. Varnek and G. Wipff, *J. Inclusion Phenom. Macrocyclic Chem.*, 2004, **49**, 47.
10 K. Matloka, A. Gelis, M. Regalbuto, G. Vandegrift and M.J. Scott, *Sep. Sci. Technol.*, 2006, **41**, 2129.
11 D. Janczewski, D.N. Reinhoudt, W. Verboom, C. Hill, C. Allignol and M. Duchesne, *New J. Chem.*, 2008, **32**, 490.
12 M.P. Jensen and A.H. Bond, *J. Am. Chem. Soc.*, 2002, **124**, 9870.
13 D. Magnusson, B. Christiansen, M.R.S. Foreman, A. Geist, J.P. Glatz, R. Malmbeck, G. Modolo, D. Serrano-Purroya and C. Sorel, *Solv. Extr. Ion Exch.*, 2009, **27**, 97.
14 M. Galletta, L. Baldini, F. Sansone, F. Ugozzoli, R. Ungaro, A. Casnati and M. Mariani, *Dalton Trans.*, 2010, **39**, 2546.
15 N.I. Nikishkin, J. Huskens, J. Assenmacher, A. Wilden, G. Modolo and W. Verboom, *Org. Biomol. Chem.*, 2012, **10**, 5443.
16 N.I. Nikishkin, J. Huskens, S.A. Ansari, P.K. Mohapatra and W. Verboom, *New J. Chem.,* 2013, **37**, 391.
17 X. Sun, H. Luo and S. Dai, *Chem. Rev*. 2012, **112**, 2100.
18 I. Billard, In *Handbook on the Physics and Chemistry of Rare Earths*, J-C.G. Bunzli and V. Pecharsky (Eds), Elsevier Science Pub. B.V., Amsterdam, 2013. **Vol. 43**, Page 213.
19 P. Gans, A. Sabatini and A. Vacca, T*alanta*, 1996, **43**, 1739.
20 P. Gans, A. Sabatini and A. Vacca, A. *J. Solution Chem.*, 2008, 37, 467.
21 P.P. Barthelemy and G.R. Choppin, *Inorg. Chem.*, 1989, **28**, 3354.
22 V. Mazan, I. Billard and N. Papaiconomou, *RSC Adv.*, 2014, **4**, 13371.
23 S.A. Ansari, L. Liu, P.D. Dau, J.K. Gibson and L. Rao, *RSC Adv.*, 2014, **4**, 37988.
24 S.A. Ansari, L. Liu and L. Rao, *Dalton Trans.*, 2015, DOI: 10.1039/c4dt03479a.

Graphical abstract